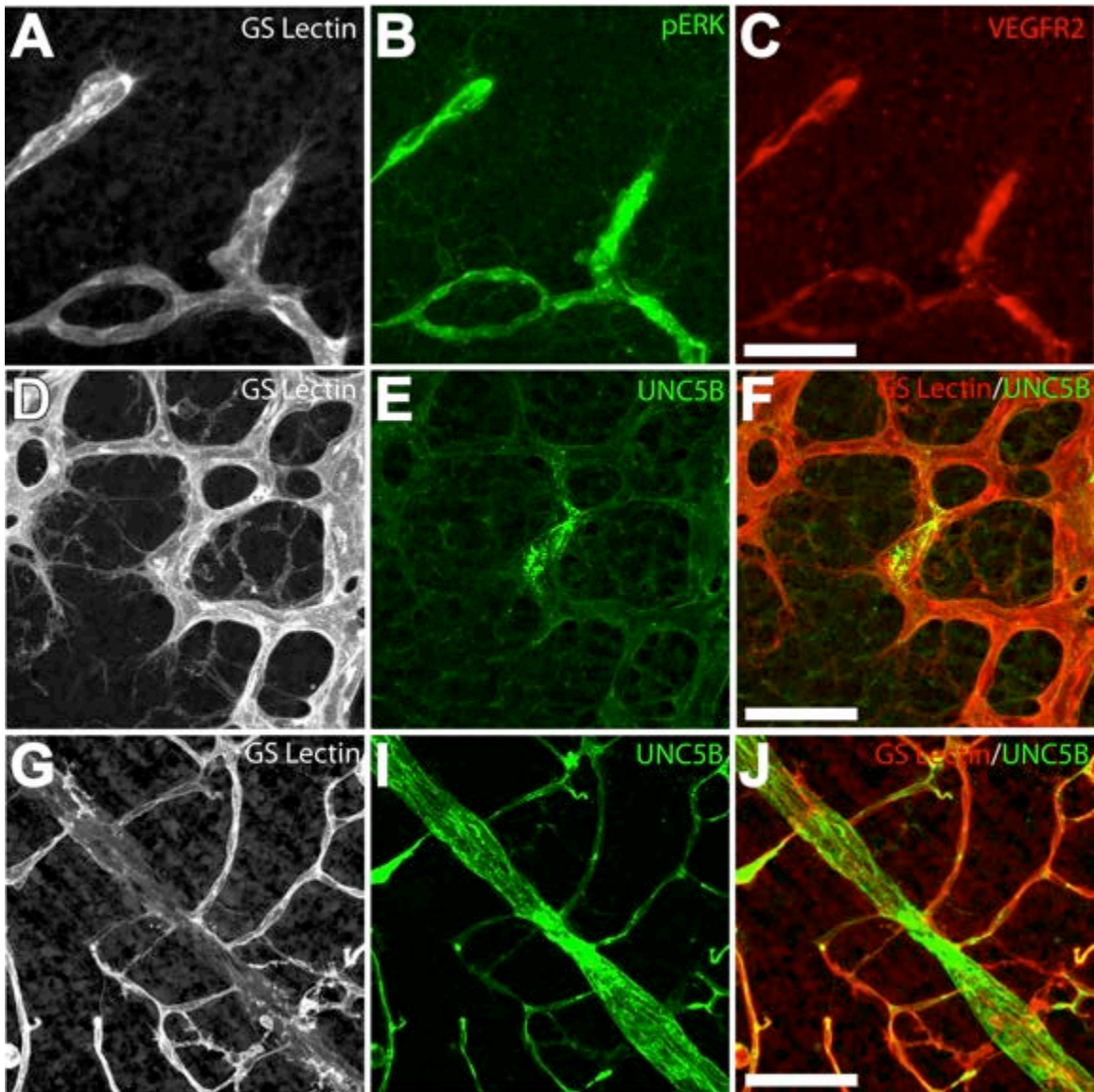


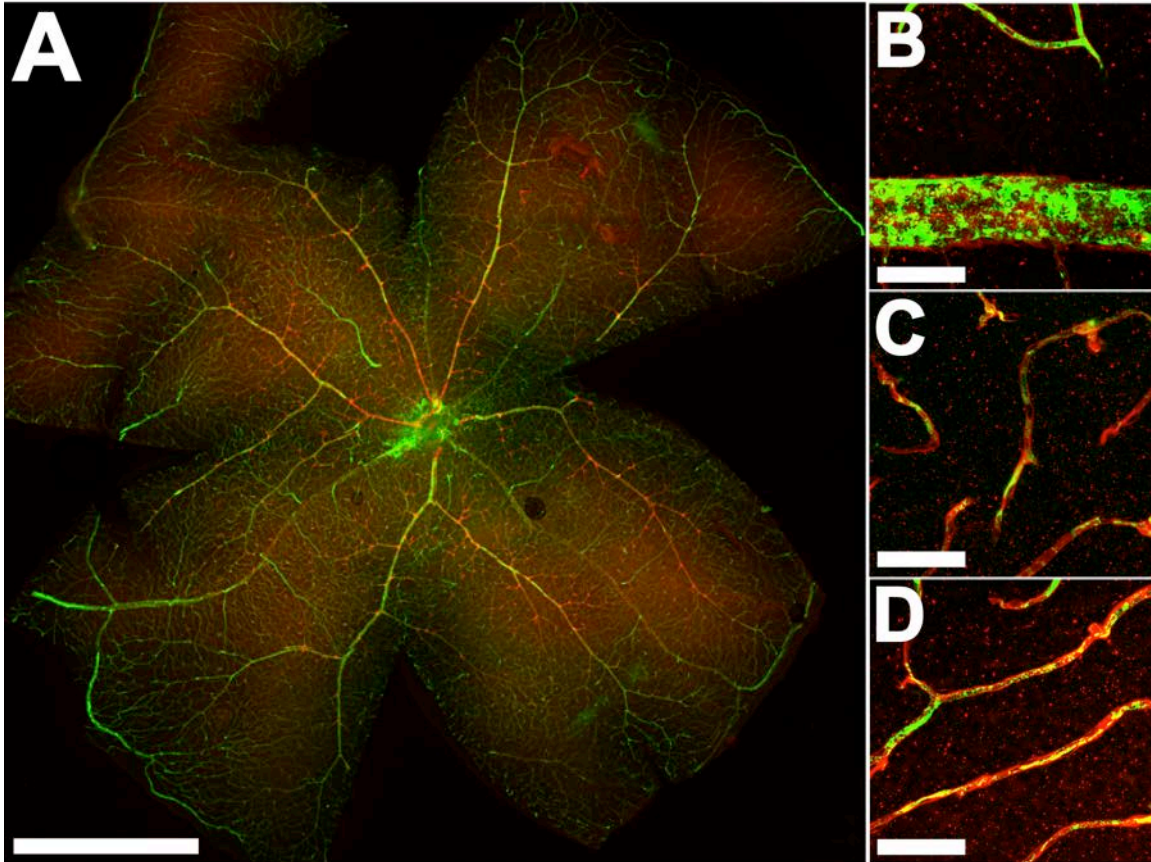
SUPPLEMENTARY MATERIAL

Stage	Plexus Layer	RasGAP Expression
P4	Super	Not in tip cells, weak in central vessels
P6	Super	Not in tip cells, weak in central vessels
P10	Super/Deep	Not in tip cells, weak in central vessels
P12	Super/Int/Deep	Deep>Superficial Plexus. Weak in Int layer
P16	Super/Int/Deep	Deep>Superficial Plexus. Weak in Int layer
P20	Super/Int/Deep	Deep>Intermediate>Superficial
Adult	Super/Int/Deep	Equally strong in all plexus layers

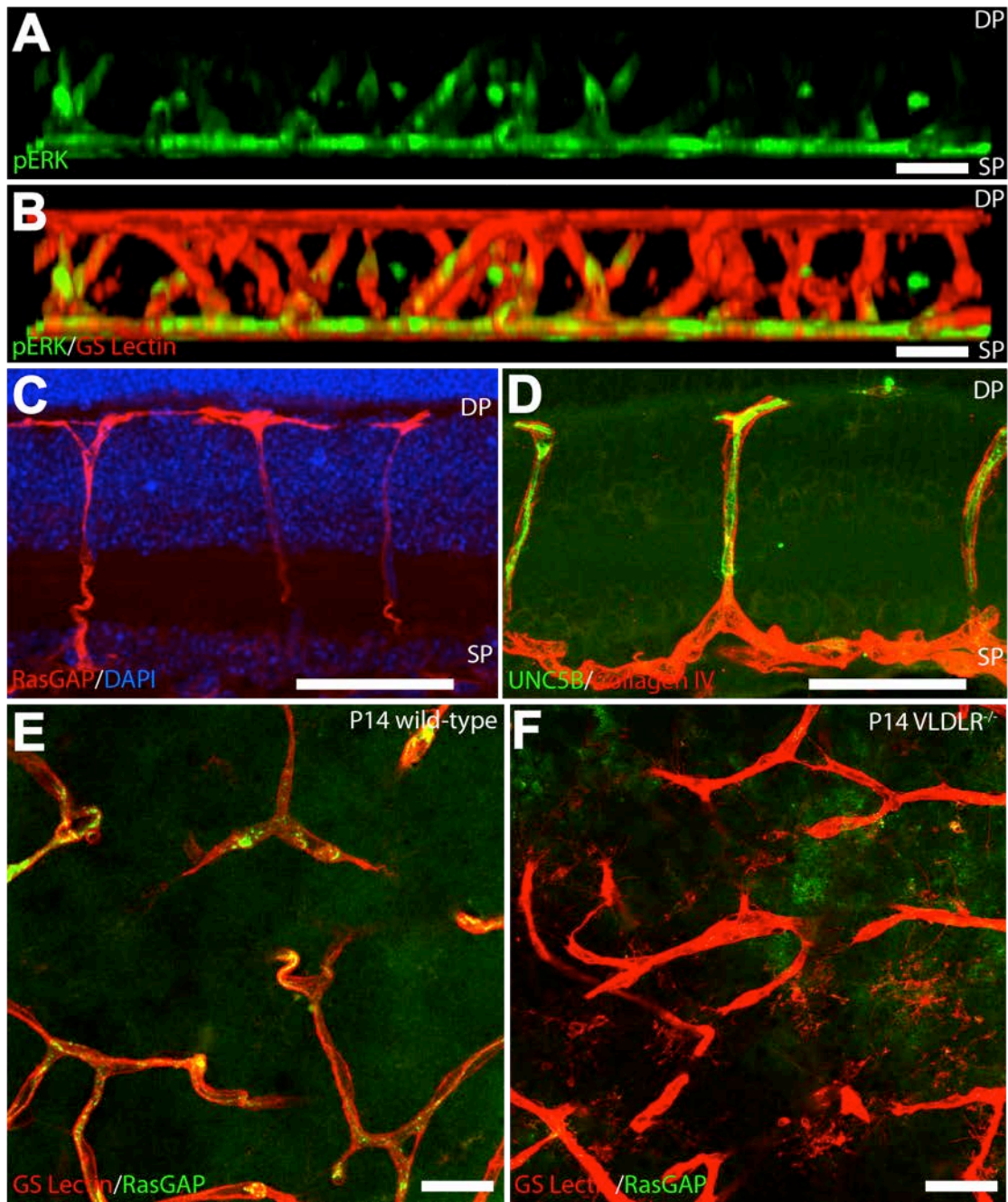
SI Table 1. Summary of RasGAP spatial localization patterns at key time-points of retinal angiogenesis. Abbreviations: super=superficial plexus, Int=intermediate plexus, deep=deep plexus.



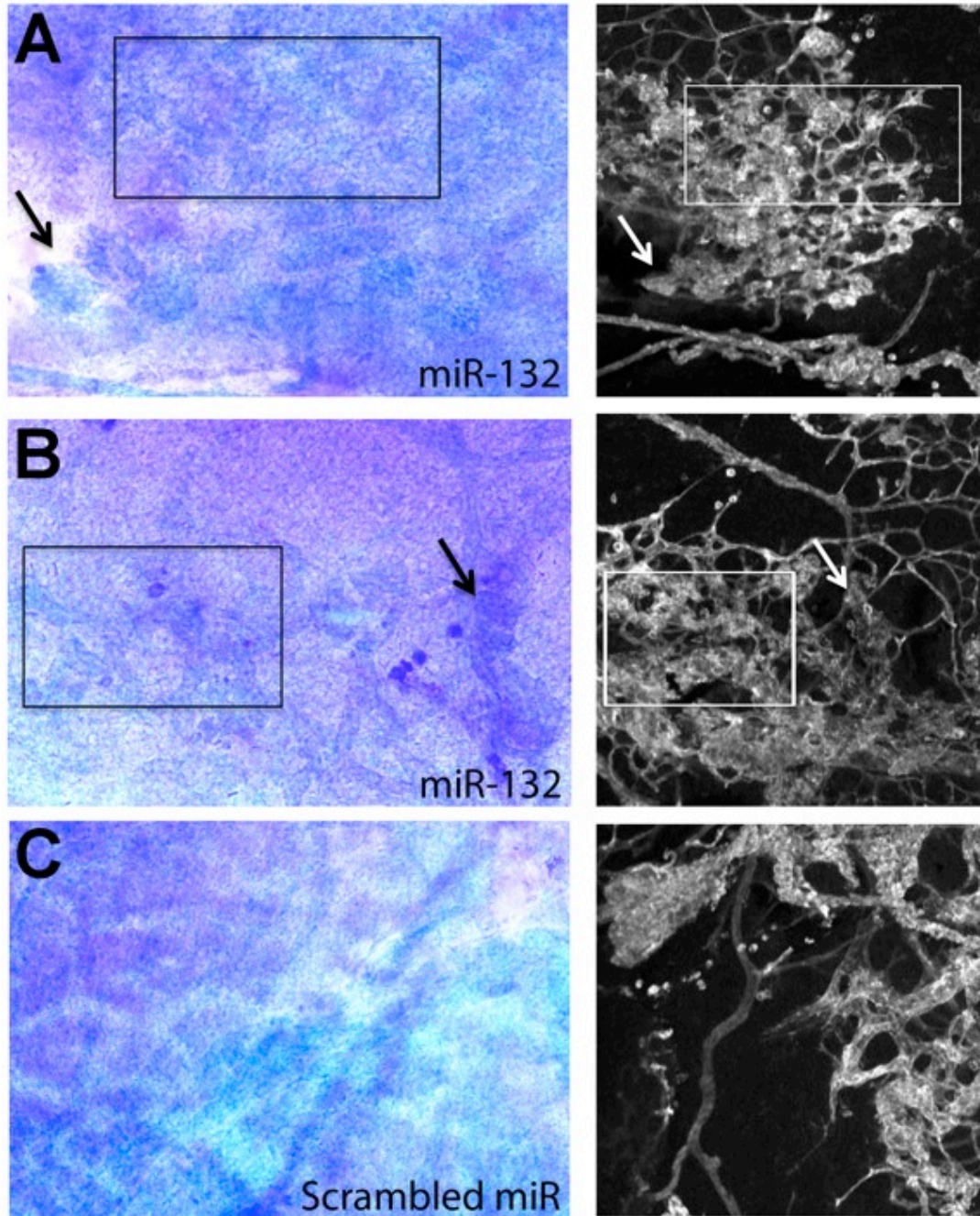
SI Fig 1. pERK and RasGAP expression patterns correlate with known sprouting and non-sprouting endothelial cell markers respectively. (A-C) Retinas from P13 OIR mice were flat-mounted and stained with GS Lectin (A), pERK (B), and the known tip cell marker VEGFR2 (C). (D-J) Retinas from P7 wild-type mice were flat-mounted and stained with GS Lectin and the known non-sprouting tip cell marker UNC5B. Fields of view containing tip cells (D-F) and quiescent cells (G-J) were imaged. Scale bars=50 μ m.



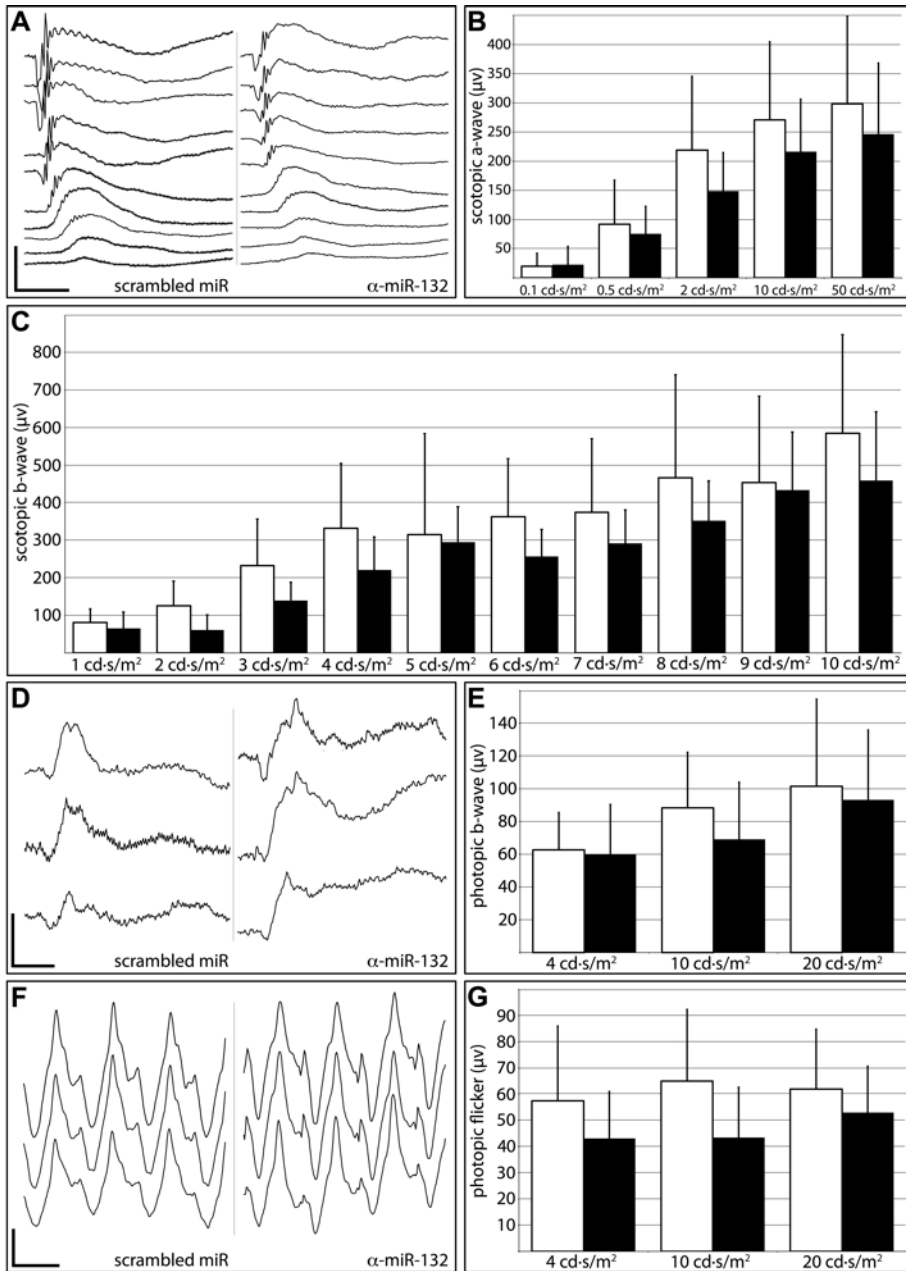
SI Fig 2. RasGAP is detected in a mosaic pattern in all blood vessels of the adult retinal vasculature. (A) RasGAP (green) and lectin (red) signals colocalize in adult retinas prepared as flat-mounts. (B-D) RasGAP is detected in blood vessels in the superficial plexus (B), intermediate plexus (C), and the deep plexus (D). Scale bars=1mm for (A), and 50 μ m for (B-D).



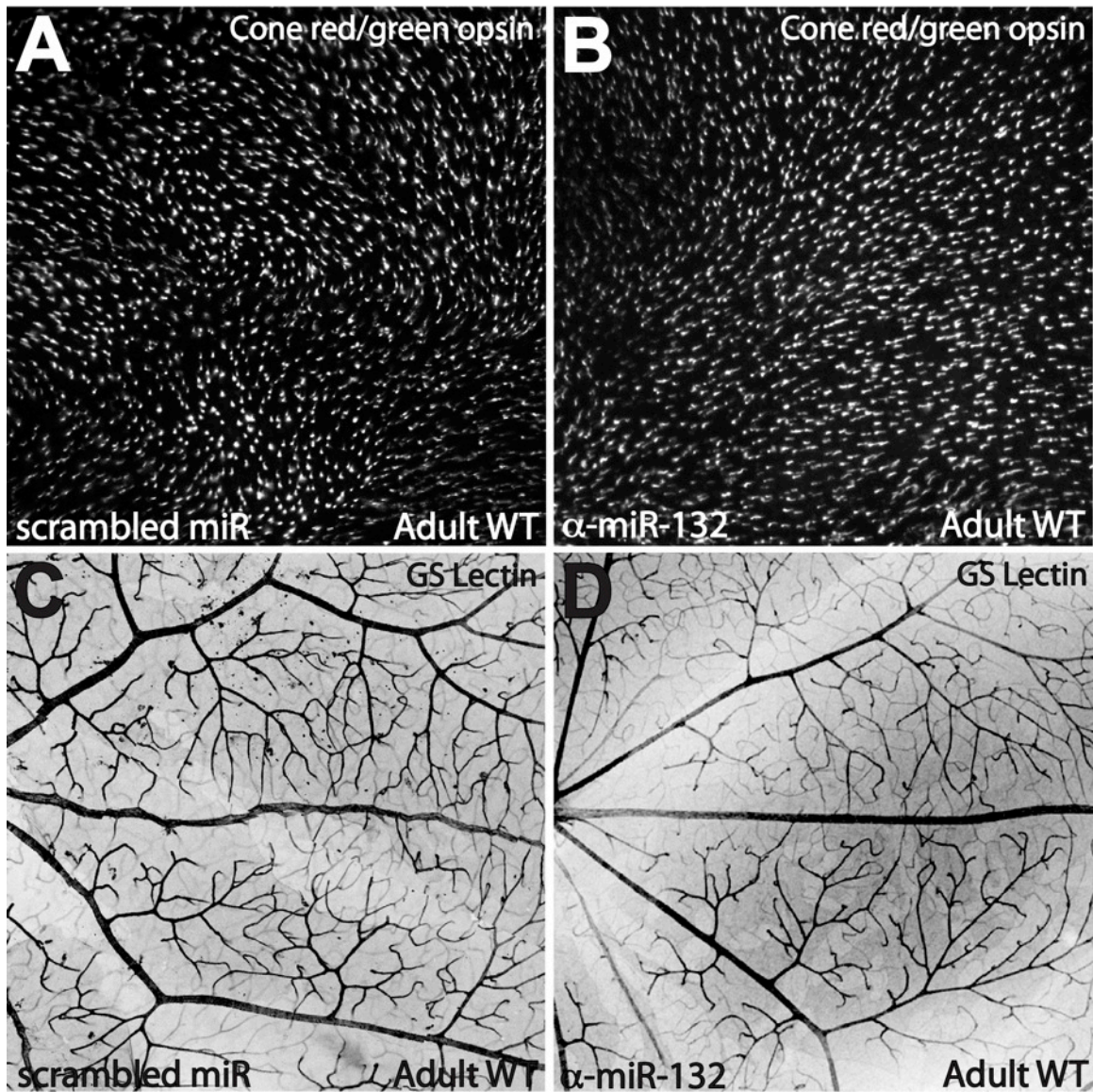
SI Fig 3. RasGAP and pERK expression in the deep plexus of the retinal vasculature. (A,B) pERK (green) is detected in the superficial plexus (SP) of P12 developing retinal vascular networks but not in the deep plexus (DP). (C) Conversely, RasGAP (red) is detected at high levels in the DP but in low levels in the SP. (D) UNC5B (green) is also detectable in the DP. RasGAP is abundant in the deep plexus of P14 wild-type (E) but not in VLDLR^{-/-} mice (F). Scale bars=50 μ m.



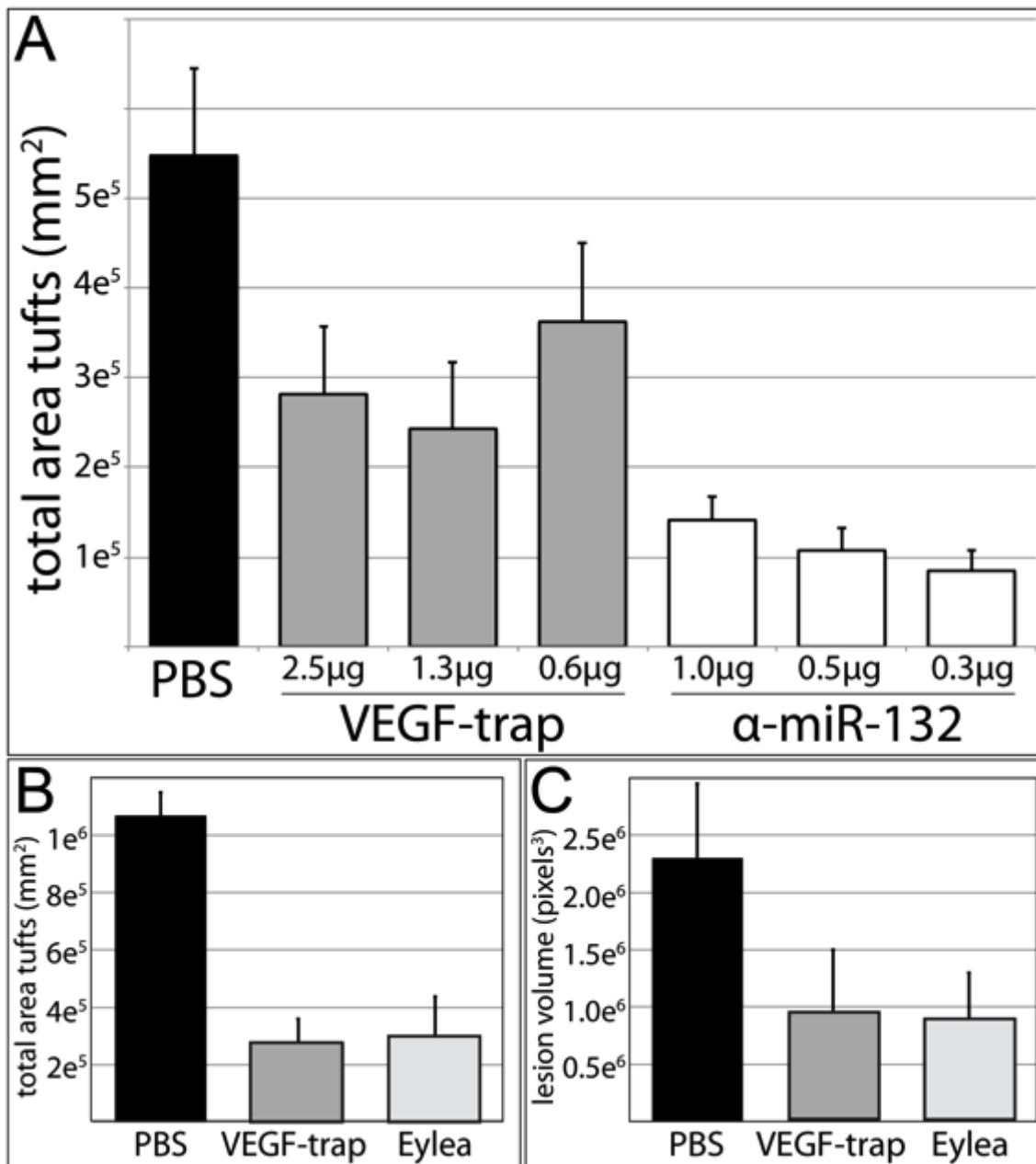
SI Fig. 4. (A,B) In situ hybridization with α -miR-132 probes of P18 OIR mice co-labeled with GS lectin reveal low miR-132 expression in the neovascular tufts. (C) Scrambled probes were also used as controls. The images on the left were taken with a different camera as the pictures on the right. The boxes mark the same region in the superficial plexus. The arrows mark regions where miR-132 expression is expressed at detectable levels. We used different cameras with different fields of view to capture the images in the left and right panels. The same sections were imaged and rectangles were drawn over the panels where the images most likely overlap.



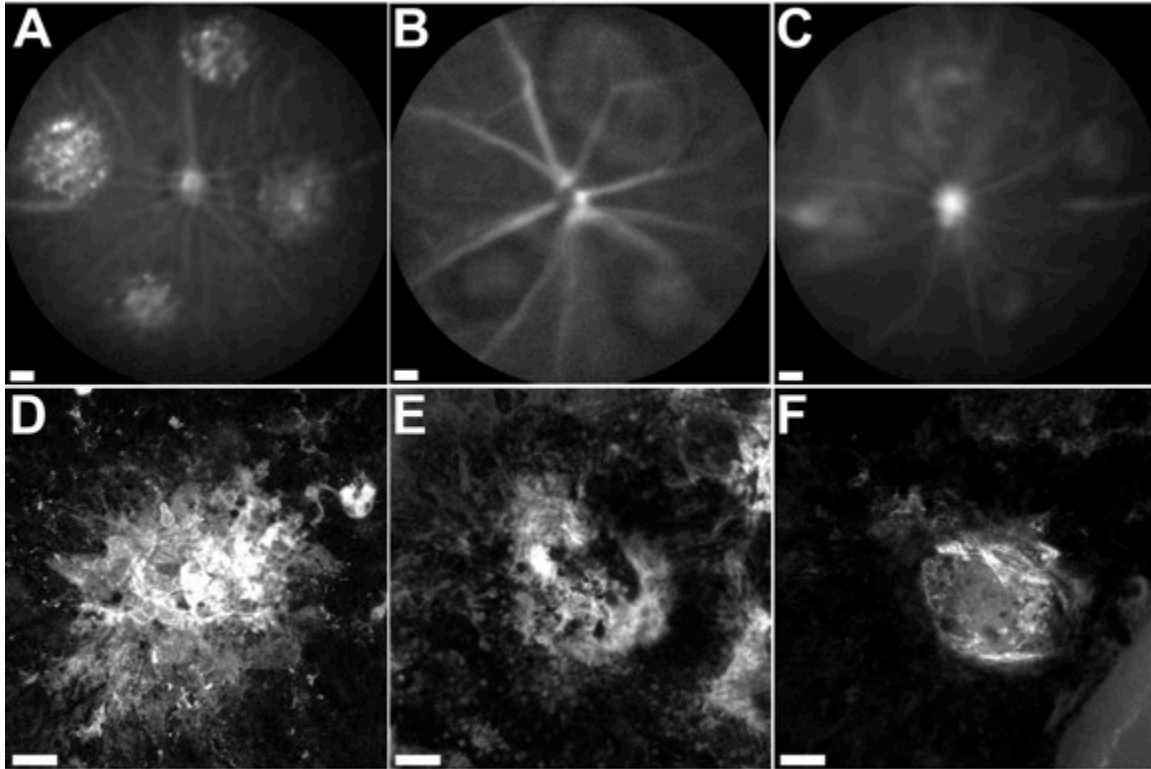
SI Fig. 5. Rod and cone photoreceptor function is preserved four days post injection of α -miR-132. (A-C) Electroretinography analyses performed four days post injection of scrambled miR or α -miR-132 in wild-type adult mice reveal that no significant differences in scotopic a-waves (B) or scotopic b-waves are elicited by the treatment. (D-G) No significant differences are observed between photopic b-waves (E) or flicker responses (G) in scrambled miR or α -miR-132 injected eyes of the same animals ($n=6$). Scale bars in panel A=0.5mv (vertical) and 100msec horizontal; in panels D&F=50 μ v (vertical) and 50msec horizontal.



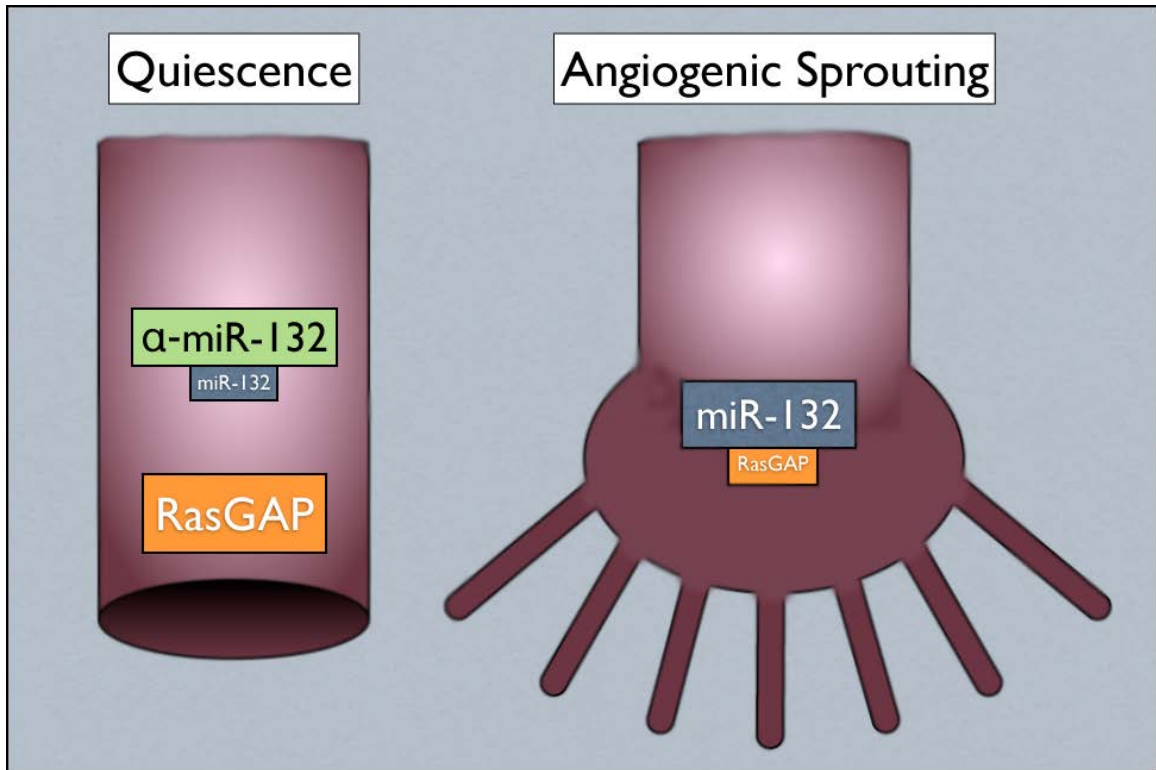
SI Fig. 6. No gross deficits to the existing vasculature or cone density are observed after α -miR-132 injections. (A&B) Retinal flat-mounts labeled with cone red/green opsin six days post injection of scrambled miR (A) or α -miR-132 (B) in wild-type adult mice are nearly indistinguishable. (C&D) The same retinas were also stained with GS Lectin to label the vasculature. No obvious differences could be observed in scrambled miR (C) or α -miR-132 injected retinas (D).



SI Fig. 7. (A) Dose response experiments comparing the ability of VEGF-trap and α -miR-132 to prevent neovascular tuft formation in P17 OIR mice. (B) VEGF-trap and Eylea α -angiogenic activities were directly compared in OIR (left) and after laser CNV (right). No significant difference was elicited after injection of the same dose of either drug for preventing tuft formation or vaso obliteration. (C) No difference was also observed after laser injury and treatment with either drug.



SI Fig 8. Lesions incurred from photocoagulation are smaller due to VEGF-trap or α -miR-132 treatments. (A-C) In vivo ICG angiography of the RPE/Choroid obtained with a cSLO one week after laser radiation. (D-F) Images of the lesions from flat-mount RPE/choroid preparations of neural retinas were captured using a confocal microscope. Z slices were obtained from the lesions and used to generate the 3D images in Fig. 7. (A,D) PBS injected; (B,E) VEGF-trap injected; (C,F) α -miR-132 injected. Scale bars=1mm for (A-C), and 50 μ m for (D-F).



SI Fig 9. Cartoon depicting the miR-132-mediated angiogenic switch in the retina. (Left) Endothelial cells are quiescent when RasGAP levels are high and miR-132 levels are low (either by endogenous downregulation or when targeted by α -miR-132). (Right) Angiogenic sprouting occurs when miR-132 attenuates RasGAP.